Correction of Susceptibility Artifacts in Slice Selective Mr Imaging at a Specific Slice Orientation Angle

K-J. Jung[1,2], and C-H. Moon[3]

[1]Brain Imaging Research Center, Univ. of Pittsburgh & Carnegie Mellon Univ., Pittsburgh, PA, United States, [2]Bioengineering Department, University of Pittsburgh, Pittsburgh, PA, United States, [3]Department of Radiology, School of Medicine, University of Pittsburgh, Pittsburgh, PA, United States

Introduction: The magnetic field inhomogeneity produced by susceptibility induces two major imaging artifacts in slice selective MR imaging; 1) the slice offset and 2) the readout shift (Fig. 1A)[1,2]. These two effects result in the geometric distortion and abnormal image intensity around the object with susceptibility. It was reported that these artifacts could be reduced by changing the slice orientation in particular in EPI 3,4. The effect of the slice orientation on the susceptibility artifacts, however, has not been analyzed to seek a slice orientation angle at which the artifacts can be corrected. By reviewing the susceptibility effect analytically, it has been discovered that there indeed exists a slice orientation angle at which the susceptibility artifacts can be corrected independent of the polarity and amplitude of the susceptibility.

Theory: Let us consider that the long axis of the cylindrical object with magnetic field inhomogeneity $h(x,z)$ is aligned along the slice axis (*z*) (Fig. 1A). The position of the selected slice is offset by $a = -h(x,z)/G_z$ in the *z* axis and the pixel is shifted by $b = h(x,z)/G_x$ in the readout (*x*) axis, where G_z and G_x are the slice and readout gradient amplitudes, respectively. In the oblique slice orientation, the readout and slice coordinates (*u*-*w* axes) are rotated by θ from *x*-*z* axes (Fig. 1B). The selected slice is offset by $a = -h(x,z)/G_w$ in the *w* axis (G_w: the slice gradient amplitude) and its coordinate on the readout axis (*u*) is dislocated to $a\tan\theta$. If the readout shift $b = h(x,z)/G_u$ can compensate for $a\tan\theta$, then its projection onto the *u* axis will not overlap with other homogenous regions in the *u* axis. Therefore, the oblique angle for the inhomogeneity correction is determined as $\theta = \tan^{-1}(G_w/G_u)$. Note that this correction angle is independent of the local inhomogeneity $h(x,z)$. The same effect should be expected for a straight slice orientation when the object is rotated at the same angle but in the opposite polarity.

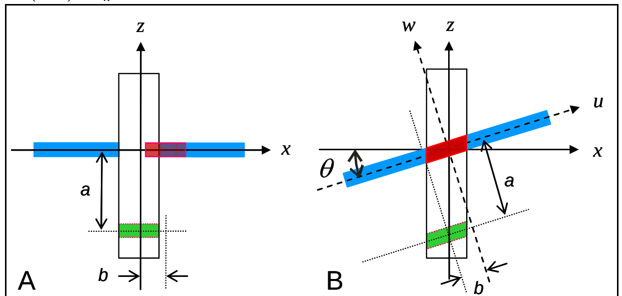

Fig. 1. Schematics of slice selection and readout in the transverse slice orientation. (A) A straight transverse. The slice axis (*z*) is parallel to the long axis of the object. The readout axis is *x*. (B) An oblique transverse. The slice axis (*w*) is oblique to the cylinder. The readout axis is *u*. *a* is the slice offset and *b* is the readout shift. The blue and green rectangles are the selected slice for the homogeneous and inhomogeneous objects, respectively. The red rectangles denote the projection of the green rectangles onto the readout axis by the frequency encoding of the readout.

Methods: The theory was confirmed by a computer simulation that calculated the spin dynamics of the spin echo (SE) sequence numerically by use of the Bloch equation and the inhomogeneity modeling of the cylinder with susceptibility[5]. The theory was also experimentally confirmed at 3T with a phantom and a human head for the straight and oblique sagittal slice of a multi-slice SE sequence. An MRI multi-purpose phantom was filled with water doped with $NiSO_4$ and NaCl. Glass vials filled with vegetable oil and air were inserted into the phantom to induce susceptibility (Fig. 2A). The axis of the cylindrical phantom was parallel to that of the glass vials. The cylinder axis of the phantom was positioned along the x axis, i.e., in a straight sagittal orientation, so that the cylinder axis of the glass vials was perpendicular to the main magnetic field direction (*z*). The readout and phase-encoding were applied along the *z* and *y* axes, respectively. The imaging parameters were FOV = 224×224 mm^2, pixel bandwidth = 224 Hz, and TR/TE = 200/16 ms. The imaging was repeated with different slice thicknesses of 8, 6, and 4 mm at the corresponding oblique angles (θ from *z* to *x*) of 14.0°, 18.4°, and 26.6°, respectively. To explore the slice tilting effect further, the phantom was rotated by 14° from the *z* axis to the –*x* axis and a straight sagittal slice was acquired at the slice thickness of 8 mm. Since the skull and scalp of the human head form a dome shape, the same effect as with the rotated phantom was expected at the lateral surface of the head, where the skull and scalp were oblique to the sagittal plane. The subject was scanned at the slice thickness of 8 mm and a slice gap of 1.6 mm at TR = 400 ms in the straight sagittal orientation.

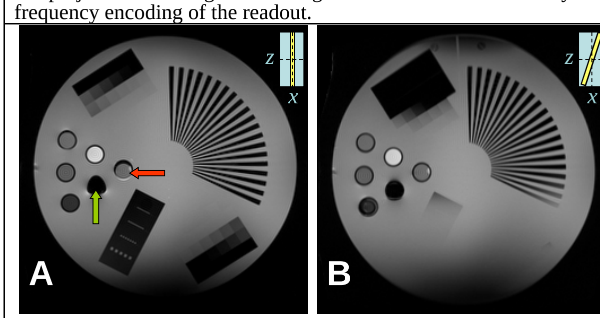

Fig. 2. Phantom images. The phantom was placed at a straight sagittal orientation. (A) A straight slice orientation. (B) An oblique slice orientation with 14° from the *z* axis toward the *x* axis. The insert in each slice represents the orientation of the phantom (a larger rectangle) and the slice angle (a smaller yellow rectangle). The vegetable oil and air are indicated by a red and green arrow, respectively.

Results: The inhomogeneity correction was successfully demonstrated in both the computer simulation and experiments. In the phantom study, the regular SE sequence produced geometric distortions at the vials containing vegetable oil ($\Delta\chi \approx -3.2$ ppm) and air ($\Delta\chi \approx 2.5$ ppm) (Fig. 2A). As expected from the mathematical analysis and computer simulation, the geometric shift due to susceptibility was corrected in the oblique slice for the straight phantom (Fig. 2B) as well as in the straight sagittal slice for the rotated phantom (not shown). The above results were reproduced at slice thicknesses of 6 mm and 4 mm. In the human head imaging, the subcutaneous fat of the scalp served as a good indicator of the presence of geometric shift due to a chemical shift (Fig. 3). The scalp appeared as double layers at the middle and left lateral sides of the head due to the readout shift of the subcutaneous fat (slice 5 and above in Fig. 3). On the other hand, the scalp on the right lateral side of the head (slice number 3 and its adjacent slices in Fig. 3) appeared as a single layer with sharper outlines. In conclusion, the susceptibility artifacts can be corrected in the slice selective imaging when the slice orientation is oblique to the long axis of the object with susceptibility by an angle of $\tan^{-1}(GS/GR)$ for the slice (GS) and readout (GR) gradient amplitudes.

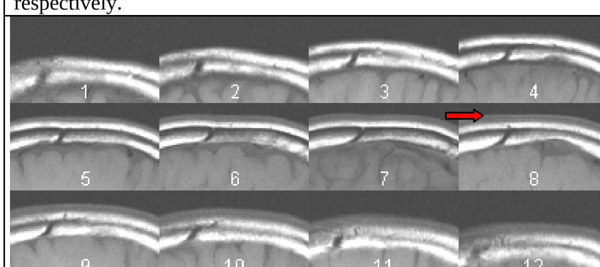

Fig. 3. Human head images. Only the superior portion of the head is shown. The numbers denote the slice index from right to left lateral side of a head. The red arrow indicates the subcutaneous fat.

References: 1. Ludeke KM, et al. Magn Reson Imaging 1985;3(4):329-343. 2. Reichenbach JR, et al. J Magn Reson Imaging 1997;7(2):266-279. 3. Deichmann R, et al. Neuroimage 2003;19(2 Pt 1):430-441. 4. Ojemann JG, et al. Neuroimage 1997;6(3):156-167. 5. Boxerman JL, et al. Magn Reson Med 1995;34(4):555-566.